Research and Reports on Metals

Research Article

New MoWHfZrTi Refractory High Entropy Alloy System: A Microstructural Verification of Phase Formation Criteria Approach

Karantzalis AE*, Poulia A*, Georgatis E, Petroglou D and Mathiou C

Abstract

The evaluation of different prediction models concerning phase formation criteria in high entropy alloys is attempted in this work. The correlation between the theoretical data and the preliminary microstructural features of MoWHfZrTi system was used as an example to further analyse the received microstructural characteristics. Based on the obtained findings, the micro segregation in the examined system was explained in terms of atomic size difference, enthalpy values, melting temperature variations and possible effects of electronegativity as derived from the prediction models. A qualitative consideration, underlying the received microstructure based on the aforementioned evidence is formulated.

Introduction

High entropy alloys (HEAs) are a new research breakthrough in metal materials technology. This novel alloy design concept has dynamically entered the scientific field and changed the past considerations. HEAs contain at least five principle elements with equi-atomic or near equi-atomic concentrations between 5-35 at.% [1]. The idea behind this definition is that compositional complexity may not necessarily lead to microstructural complexity, due to the influence of entropy.

Specifically, the high-entropy effect originates from the significantly higher configurational entropy in these systems compared to that in conventional alloys. Such high mixing entropy can favour the formation of disordered solution states and suppress the formation of intermetallic compounds, which is of paramount importance in the applications of these materials [2,3].

Up to date, numerous compositions of HEAs based on transition elements such as Co, Cr, Fe, Ni as well as Al and Cu have been examined, resulting in a large variety of microstructures (e.g. simple fcc and bcc solid solution phases, typical dendrite and interdendrite structures, morphology transitions from dendrites to equi-axed grains, spinodal decomposition tissues etc.) [4-9].

All these systems were also found to exhibit intriguing properties, including superb specific strength, excellent mechanical performance, exceptional ductility and fracture toughness at cryogenic temperatures [10-13]. For instance, new light alloy families based on elements such as Al, Be, Li, Mg, Sc, Si, Sn, Ti and Zn, can be used in the transportation industry and energy sectors, where lightweight high-strength materials are in great demand [14].

In view of these optimistic findings, more HEAs with promising properties can be discovered with further advancements, thereby promoting the applications of metallic materials in industries which were previously limited. However, in recent years there has been a pressing need to develop the next-generation materials suitable for applications with high melting point requirements. Towards this direction, the use of refractory metals and more specifically the refractory high entropy alloy (RHEAs) systems are considered to be among the possible candidates for such efforts [15-17].

From 2010 onwards, several studies have been pursued to explore new HEAs based on refractory constituents. RHEAs usually possess excellent mechanical properties at high temperatures, thermal stability and wear resistance together with satisfying oxidation performance [18-21].

As all these unique properties of HEAs mostly originate from the formation of multi-component solid solutions, it is of vital need to understand the rules governing the formation of such phases in HEAs. Towards this direction, the alloy design for equi-atomic multi-component alloys was rationalized by statistically analyzing the atomic size difference, mixing enthalpy and mixing entropy values among the constituent elements in solid solutions forming high entropy alloys [22].

In order to form solid solution phases (i.e. fcc, bcc and their mixtures, including both ordered/disordered phases), the following conditions have to be met simultaneously: $\delta \leq 8.5$, $-22 \leq \Delta H_{mix} \leq 7$ kJ/mol and $11 \leq \Delta S_{mix} \leq 19.5$ J/(K·mol).

These three parameters are defined by Eqs (1-3) respectively:

$$\delta = 100 \sqrt{\sum_{i=1}^{n} c_i (1 - r_i / \bar{r})^2} \tag{1}$$

where $\bar{r} = \sum_{i=1}^{n} c_i r_i$, c_i and r_i are the atomic percentage and atomic radius of the ith element. The numerical factor 100 is used to amplify the data for clarity;

$$\Delta H_{mix} = \sum_{i=1, i \neq j}^{n} \Omega_{ij} c_i c_j \tag{2}$$

where $\Omega ij = 4\Delta H_{mix}^{AB}$, ΔH_{mix}^{AB} is the mixing enthalpy of binary liquid AB alloys; and

$$\Delta S_{mix} = -R \sum_{i=1}^{n} c_i \ln c_i \tag{3}$$

where R is the gas constant.

*Corresponding author: Karantzalis AE, Department of Materials Science and Engineering, University of Ioannina, 45110 Ioannina, Greece, E-mail: akarantz@cc.uoi.gr

Poulia A, Department of Materials Science and Engineering, University of Ioannina, 45110 Ioannina, Greece, E-mail: apoulia@cc.uoi.gr

Recently, a new model that predicts the specific combinations of elements most likely to form single-phase high entropy alloys, was introduced by Troparevsky et al. [23]. The model correctly identifies all known single-phase alloys, while rejecting similar elemental combinations that are known to form an alloy comprising multiple phases. This method focuses on the use of high-throughput computation of the enthalpies of formation (ΔH^f) of binary compounds in HEAs systems. The model suggests the formation of simple solid solutions with the ΔH^f values of the binary components escalating inside the recommended boundaries for single-phase solid solution formation (-232 < ΔH^f < 37 meV/mol) regarding a 5 component refractory high entropy alloy.

Lastly, an additional method for rapidly predicting the formation and stability of undiscovered single phase HEAs has been developed, using Miedema's model as a basis [24]. The introduction of a new parameter, Φ, suggests the formation of stable solid solutions at the systems' melting temperature (using www.alloyASAP.com platform as a calculation tool). Of the 185 alloys used to benchmark this new method, 16 exceptions were found, indicating a drive for ordering on the atomic scale, as verified by DFT analysis. The Φ factor adopted by King et al. [24] incorporates the thermodynamic factors of ΔG_{ss} that is the change in Gibbs free energy for the formation of a fully disordered solid solution from a mixture of its individual elements and ΔG_{max} which is the lowest (intermetallic) or highest (segregated) possible Gibbs free energy obtainable from the formation of binary systems from the constituents of the mixture. These two values are combined to form the new parameter, $\Phi = \Delta G_{ss}/-|\Delta G_{max}|$. According to the proposed model, a value of $\Phi \geq 1$ would suggest a stable

solid solution at the systems' melting temperature, while a negative value of Φ recommends that the solid solution has a positive formation enthalpy and will not form.

In any case, the use of all of all these prediction models is a first theoretical asset in trying to understand the complexity of high entropy alloys. Undoubtedly, careful experimental assessment of HEAs is necessary before conclusions are drawn about the characteristics and stabilities of the final microstructures. Therefore, research effort should focus on alloys that possess the desired balance of microstructural features and crucial properties.

Materials and Methods

$Mo_{0.95}W_{0.95}Hf_{1.0}Zr_{1.1}Ti_{1.1}$ high entropy alloy was prepared by vacuum arc melting of near equi-molar mixtures of the corresponding elements. The raw materials were in the form of powders or wires (in the case of Zr) with a purity of over 99.5% each. Arc melting of the alloy was conducted on a water-cooled copper plate in an atmosphere of high purity argon. To improve the distribution of elements in the alloy, the samples were re-melted seven times and flipped for each melt. Standard metallographic procedure was subsequently adopted in order to prepare the samples for the following characterization steps.

Different phase formation criteria mentioned before were calculated, regarding the specific alloy in a wider attempt to correlate theoretical prediction evidence with microstructural observations. More specifically, estimations of atomic size difference, enthalpy of mixing, entropy of mixing, enthalpy of formation and Φ parameter data were evaluated and compared with the received morphological findings.

The crystal structure of the alloy was examined with an X-ray diffractometer (Bruker, D8 Advance) using a scanning rate of 0.01º/ sec, while its actual microstructure was further analyzed with the use of a Scanning Electron Microscope (JEOL 6510 LV) equipped with both backscatter electron (BSE) and energy dispersive spectroscopy (EDS) detectors.

Results

Prediction models based evaluation of the $Mo_{0.95}W_{0.95}Hf_{1.0}Zr_{1.1}Ti_{1.1}$ system

According to the data of Table 1, the calculated parameters of the examined system, appear to satisfy the conditions for single solid solution formation proposed by Guo et al. [22] as δ = 6.8, ΔH_{mix} = -5.55 kJ/mol and ΔS_{mix} = 13.36 J/K·mol, all lying within the proposed value ranges mentioned before. The model proposed by Troparevksy et al. [23] also indicates the formation of a simple solid solution with the ΔH^f values of the binary components escalating inside the recommended extended boundaries for single phase solid solution formation in refractory systems. Finally, the King's et al. [24] proposed model, gives values for δ and Φ equal to 6.136 and 1.312 respectively, which are within the safe ranges for solid solution formation (calculations were conducted using the www.alloyASAP. com platform proposed by these authors). It should be noticed, however that both the predicted δ and Φ values are very close to the marginal limits and King et al. [24] in their approach have commented on potential diversions from the expected behaviour as the values of these parameters are approaching the stability limits.

The three different models combined predictions, do not lead to an absolute and certain result on the tendency the system exerts in forming a single phase solid solution. As such, the characterization of the actually produced alloy system is necessary to further ascertain its microstructural features and behaviour.

Microstructural characterization of $Mo_{0.95}W_{0.95}Hf_{1.0}Zr_{1.1}Ti_{1.1}$ system

Figure 1 shows the XRD spectrum of the produced alloy. Clearly, the presence of different crystal structures is evident. Analysis of the spectrum indeed reveals the presence of BCC and HCP based structures, with their crystal lattice parameters included on the top-right table compacted with the diffraction pattern. These observations indicate that the system is showing a phase segregation tendency, without nevertheless, the high degree of its uncertainty in forming a single phase solid solution not having been predicted and commented by the model of King et al. [24] as both of the involved parameters (δ and Φ) are close to their proposed limits.

The evident by the XRD analysis phase segregation, is further verified by the SEM microstructural examination, presented in Figure 2. Obviously, the alloy consists of dark and bright areas, which is a strong indication of phase segregation, while the overall microstructure can be characterized as significantly refined (both bright and dark areas < 5μm).

Elemental mapping of the alloy's microstructure by EDS analysis (Figure 3) verifies the segregation of W and Mo within the bright areas and Zr and Hf within the dark areas. Ti is found to be more evenly distributed within the overall microstructure. This elemental segregation becomes further evident by line scan EDS analysis presented in Figure 4 respectively. Senkov et al. [15] and Couzinié et al. [25] have also reported and commented on significant elemental

Table 1: Calculated values of atomic size difference, enthalpy of mixing, entropy of mixing, enthalpy of formation and Φ parameter, according to different proposed prediction models.

Calculated Parameters	Guo et al. [22]			Troparevsky et al. [23]	King et al. [24]	
	δ	ΔH_{mix} [kJ/mol]	ΔS_{mix} [J/K·mol]	ΔH_f [meV/atom]	δ	Φ
$Mo_{0.95}W_{0.95}Hf_{1.0}Zr_{1.1}Ti_{1.1}$ System	6.8	-5.55	13.36	*(see embedded table below)*	6.136	1.312

Embedded table (Troparevsky ΔH_f detail):

System	δ	ΔH_{mix} [kJ/mol]	ΔS_{mix} [J/K·mol]	ΔH_{form} [meV/atom]					δ	Φ
$Mo_{0.95}W_{0.95}Hf_{1.0}Zr_{1.1}Ti_{1.1}$	6.8	-5.55	13.36						6.136	1.312

meV/atom	Mo	W	Ti	Hf	Zr
Mo	0	-8	-167	-171	-138
W	-8	0	-82	-171	-145
Ti	-167	-82	0	-10	24
Hf	-171	-171	-10	0	-22
Zr	-138	-145	24	-22	0

Energy scale (meV/atom): -500 -400 -300 -200 -100 -10 10 100 200 300

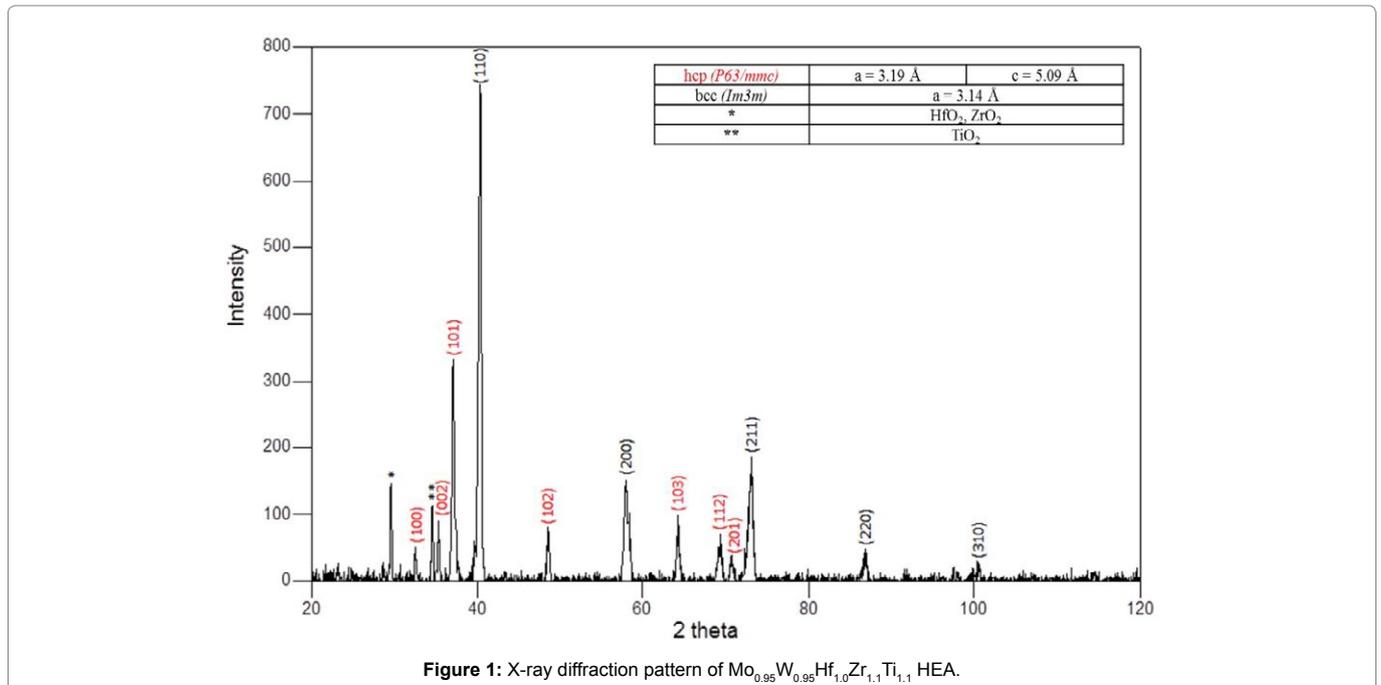| hcp (P63/mmc)	a = 3.19 Å	c = 5.09 Å
bcc (Im3m)	a = 3.14 Å	
*	HfO₂, ZrO₂	
**	TiO₂	

Figure 1: X-ray diffraction pattern of $Mo_{0.95}W_{0.95}Hf_{1.0}Zr_{1.1}Ti_{1.1}$ HEA.

segregation in their research efforts. Senkov et al. [15] associated this elemental segregation with non-equilibrium solidification conditions that result in a kinetically restricted homogeneous distribution of the involved elements within the growing solid phases. They also supported that this segregation is linked with the melting point differences of the involved elements and with the high cooling rates both of which tend to expand the liquidus-solidus area.

In order to further ascertain the behaviour of the system upon solidification, it is interesting to calculate the predictions of the King et al. [24] model for the actual formed phases of the examined alloy. Table 2 summarizes the values obtained by the www.alloyASAP.com platform for the two different phases observed in the final microstructure. It can be seen that the light phase possesses a considerably higher T_m value than the dark phase. The calculation of T_m values was conducted using the following equation

$$T_m = \sum_{i=1}^{N} x_i (T_m)_i \qquad (4)$$

where x_i and T_{mi} are the atomic percentage and the melting temperature of the ith alloy component, respectively.

This could be a strong indication that the W and Mo rich phase is the first to form upon solidification, which is in agreement with the speculations of Senkov et al. [15] on the importance of the melting point, at least on the onset of solidification. Both phases are characterized by relatively high values of Φ (2.54 for the light phase and 49.57 for the dark phase) and low values of δ (4.8 for the light phase and 3.01 for the dark phase) especially compared with the values corresponding to the initial calculations for the monolithic alloy (Table 1).

Under these observations it can be possibly suggested that the system exerts the tendency to be segregated in two phases that are
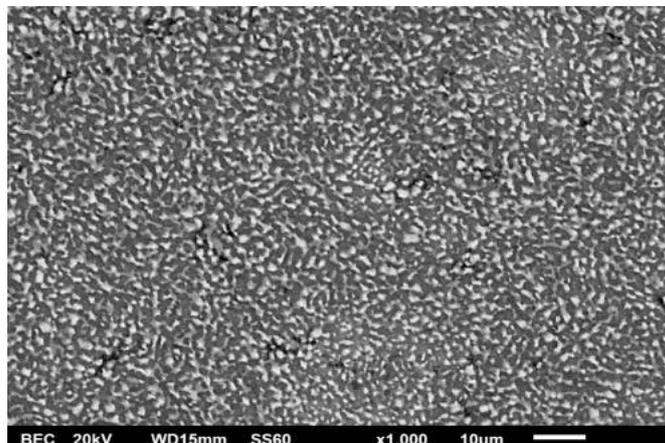
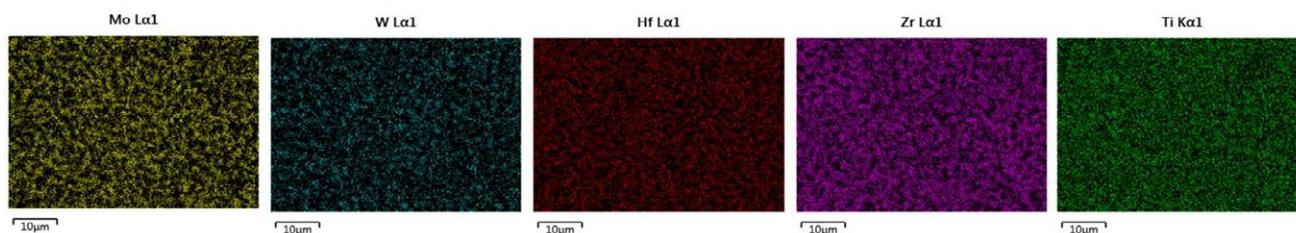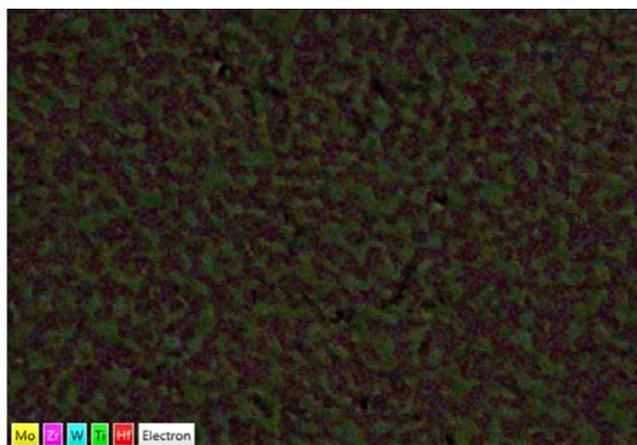**Figure 2:** SEM backscattered electron micrograph of $Mo_{0.95}W_{0.95}Hf_{1.0}Zr_{1.1}Ti_{1.1}$ HEA.

Figure 3: EDS mapping analysis of $Mo_{0.95}W_{0.95}Hf_{1.0}Zr_{1.1}Ti_{1.1}$ HEA.

characterized, by the calculated values, by a higher degree of stability. This speculation verifies the concerns expressed by Tsai et al. [26] recently and Pickering et al. [27] previously that the polyparametric simple solid solution formation models do not always mirror the actually received experimental evidences and as such, the dogmatic focusing on the formation of a single phase structure should be abandoned or at least reconsidered.

The current experimental results, hence, most likely suggest that the high melting point elements will solidify first, leading to the segregation of the low melting point elements to the lastly to solidify liquid, for reasons that are related with the distortion Hf, Zr and Ti may cause to the W-Mo lattice, as will be explained in a following paragraph. This approach does support the observations of the present effort as W and Mo with the higher melting points are located within the bright – first to solidify – areas pushing thus, Zr and Hf of lower melting points to the last stages of solidification. Ti appears to be more evenly distributed throughout the microstructure despite its even lower melting point, yet its atomic size is closer to W and Mo than Hf and Zr, a fact that could also account for its homogeneous distribution. Couzinié et al. [25] have also expressed similar thoughts on the effect of the melting points. It should be also noticed at this point that the examined sample surfaces are from the base of the meniscus, close to the water cooled copper base, i.e. from areas of high cooling rates which, according to Senkov et al. [15] approach further encourages the segregation phenomena.
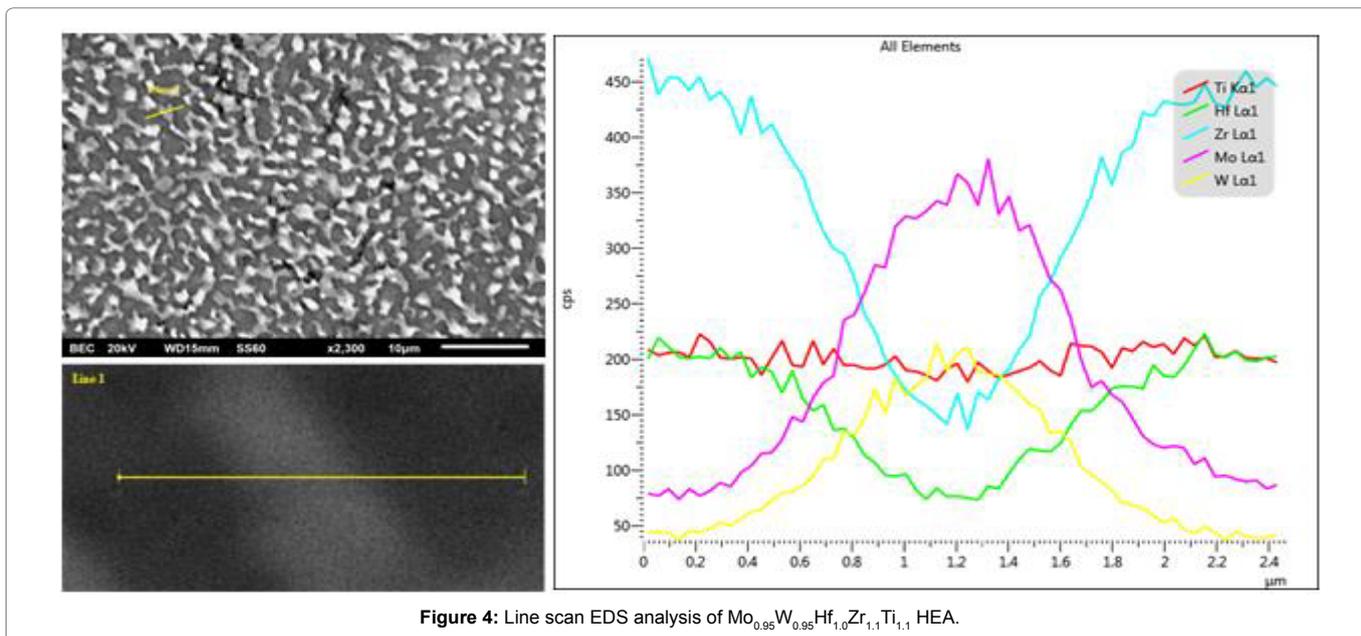
Figure 4: Line scan EDS analysis of $Mo_{0.95}W_{0.95}Hf_{1.0}Zr_{1.1}Ti_{1.1}$ HEA.

Table 2: Summarized criteria for the actual formed phases according to King's et al. [24] proposed model.

Initial alloy composition	Formed phases actual composition	Parameters calculation (using the www.alloyASAP.com platform)		
		δ	Φ	T_m [K]
$Mo_{0.95}W_{0.95}Hf_{1.0}Zr_{1.1}Ti_{1.1}$	Dark area Hf = 34.40 at.% Zr = 48.67 at.% Ti = 16.93 at.%	3.01	49.57	2226
	Light area Mo = 41.00 at.% W = 29.90 at.% Hf = 6.61 at.% Zr = 5.63 at.% Ti = 16.87 at.%	4.81	2.54	2905

Table 3: Atomic radius, pauling electronegativity and valance electron concentration values for MoWHfZrTi HEA's elements [28].

Element	Atomic radius [Å]	Electronegativity	VEC
Mo	1.363	2.16	6
W	1.367	2.36	6
Ti	1.462	1.54	4
Hf	1.578	1.30	4
Zr	1.603	1.33	4

Caution should be taken however, as the present microstructural morphologies are not similar with those obtained in the efforts of Senkov et al. and Couzinié et al. [15,25] where dendritic [15] or gradually vanishing dendritic [25] structures were observed. A rather equiaxed – especially for the primary W – Mo enriched grains – microstructure was observed, which may raise questions on the establishing for growth driving force conditions (temperature gradients, undercooling, element distribution) ahead of the solidifying fronts, as they may alter the involved segregation mechanisms. Further experimental effort is currently being undertaken by the authors.

Further expanding the solidification behaviour of the examined system, shows that Mo and W initiate the solidification phenomena, entrapping in a preceding stage Hf, Zr and Ti and indeed in an order reversely proportional to their atomic radius causing less lattice distortion (Table 3 values derived from [28]). Hence Hf and Zr that are causing the higher lattice distortion are only present to an extent of roughly 6 at.% whereas Ti, causing less lattice distortion, is present at higher proportions (around 17 at.%). Despite, hence, the fact, that all these elements are attractive to form simple solid solutions, it seems that the lattice distortion plays a predominant effect on the elemental dissolution within the primary W-Mo lattice.

It has to be mentioned, thus, once again that the low melting point elements are segregated to the lastly to solidify phase, most importantly due to the distortion they cause on the W-Mo lattice – so that they cannot be accommodated within it - rather than their actual low melting point. What their low melting point really causes is that it deprives from these elements the chance for them to initiate the nucleation – solidification process.

Finally, at this point it should be underlined that the correlation of the onset of solidification process with the alloying elements having the higher melting temperature values is not the only event that pushes the elements with the lowest melting points to the last

stages of solidification. Simultaneously, other factors (such as lattice distortion, electronegativity differences and valance electron concentration values) may possibly play a predominant role in these phenomena, making the whole process a multi-factor condition.

For example, as known, the Hume-Rothery rule which has been successfully applied to binary alloys, is not a directly applicable way to explain problems that exist for HEA systems that contain five or more principal components. Moreover, based on the rule of topological stability and chemical compatibility, the relationship between the formation of high entropy alloys and electronegativity values indicates that a lower value of electronegativity is favorable to form solid solution phases [29]. From Table 3 it seems that Ti having higher electronegativity value compared to Hf and Zr is found to be at higher proportions within the lattice of the primary light phase. This is, however, a premature speculation and further investigation is currently been undertaken in order to obtain more conclusive results towards this direction. Finally, the revealing of the effect of the Valance Electron Concentration on the phase stability of HEAs is also vitally important for further alloy design and phase selection in HEAs [30].

Conclusions

A refractory high entropy alloy MoWHfZrTi was produced by vacuum arc melting of its corresponding elements. Evaluation of the phase formation criteria concerning atomic size difference, enthalpy of mixing and entropy of mixing values provided some first clues for single solid solution formation. Two different prediction models also suggested potential phase stability, or didn't give clear evidence about the final phase selection.

As such, the actual alloy examination presented a significantly refined microstructure with indications of segregation. This phase segregation tendency was also verified by X-ray data, revealing the presence of BCC and HCP based structures.

A possible explanation of these features was attempted in order to further ascertain the behaviour of the examined system upon solidification, for the actual formed phases. The influence of melting temperature, cooling rate, atomic radius or maybe electronegativity and VEC values, are most likely associated with the observed microstructural characteristics.

References

1. Yeh JW, Chen SK, Lin SJ, Gan JY, Chin TS, et al. (2004) Nanostructured high-entropy alloys with multiple principal elements: novel alloy design concepts and outcomes. Adv Eng Mater 6: 299-303.

2. Ranganathan S (2003) Alloyed pleasures: multimetallic cocktails. Curr Sci 85: 1404-1406.

3. Yeh JW (2006) Recent progress in high entropy alloys. Ann Chim Sci Mater 31: 633-648.

4. Tong CJ, Chen YL, Chen SK (2005) Microstructure characterization of Al$_x$CoCrCuFeNi high-entropy alloy system with multiprincipal elements. Metall Mater Trans A 36: 881-893.

5. Manzoni A, Daoud H, Völkl R, Glatzel U, Wanderka N (2013) Phase separation in equiatomic AlCoCrFeNi high-entropy alloy. Ultramicroscopy 132: 212-215.

6. Zhang Y, Ma SG, Qiao JW (2012) Morphology transition from dendrites to equiaxed grains for AlCoCrFeNi high-entropy alloys by copper mold casting and bridgman solidification. Metall Mater Trans A 43: 2625-2630.

7. Zhuang Y, Liu WJ, Chen ZY, Xue HD, He JC (2012) Effect of elemental interaction on microstructure and mechanical properties of FeCoNiCuAl alloys. Mater Sci Eng A 556: 395-399.

8. Fan QC, Li BS, Zhang Y (2014) The microstructure and properties of (FeCrNiCo) Al$_x$Cu$_y$ high-entropy alloys and their TiC-reinforced composites. Mater Sci Eng A 598: 244-250.

9. Varalakshmi S, Kamaraj M, Murty BS (2010) Formation and stability of equiatomic and nonequiatomic nanocrystalline CuNiCoZnAlTi high-entropy alloys by mechanical alloying. Metall Mater Trans A 41: 2703-2709.

10. Zhang Y, Zuo TT, Tang Z, Gao MC, Dahmen KA, et al. (2014) Microstructures and properties of high-entropy alloys. Prog Mater Sci 61: 1-93.

11. Tsai MH, Yeh JW (2014) High-entropy alloys: a critical review. Mater Res Lett 2: 107-123.

12. Ye YF, Wang Q, Lu J, Liu CT, Yang Y (2016) High-entropy alloy: challenges and prospects. Mater Today 19: 349-362.

13. Yeh JW (2013) Alloy design strategies and future trends in high-entropy alloys. JOM 65: 1759-1771.

14. Miracle D, Miller JD, Senkov ON, Woodward C, Uchic MD, et al. (2014) Exploration and development of high entropy alloys for structural applications. Entropy 16: 494-525.

15. Senkov ON, Wilks GB, Miracle DB, Chuang CP, Liaw PK (2010) Refractory high-entropy alloys. Intermetallics 18: 1758-1765.

16. Senkov ON, Scott JM, Senkova SV, Meisenkothen F, Miracle DB, et al. (2012) Microstructure and elevated temperature properties of a refractory TaNbHfZrTi alloy. J Mater Sci 47: 4062-4074.

17. Gorr B, Azim M, Christ HJ, Mueller T, Schliephake D, et al. (2015) Phase equilibria, microstructure, and high temperature oxidation resistance of novel refractory high-entropy alloys. J Alloy Compd 624: 270-278.

18. Juan CC, Tsai MH, Tsai CW, Lin CM, Wang WR, et al. (2015) Enhanced mechanical properties of HfMoTaTiZr and HfMoNbTaTiZr refractory high-entropy alloys. Intermetallics 62: 76-83.

19. Poulia A, Georgatis E, Lekatou A, Karantzalis A (2017) Dry-sliding wear response of MoTaWNbV high entropy alloy. Adv Eng Mater 19: 1-10.

20. Liu CM, Wang HM, Zhang SQ, Tang HB, Zhang AL (2014) Microstructure and oxidation behaviour of new refractory high entropy alloys. J Alloys Compd 583: 162-169.

21. Tsai MH, Wang, CW, Tsai CW, Shen WJ, Yeh WJ, et al. (2011) Thermal stability and performance of NbSiTaTiZr high-entropy alloy barrier for copper metallization. J Electrochen Soc 158: 1161-1165.

22. Guo S, Liu CT (2011) Phase stability in high entropy alloys: Formation of solid-solution phase or amorphous phase. Prog Nat Sci 21: 433-446.

23. Troparevsky MC, Morris JR, Kent PRC, Lupini AR, Stocks GM (2015) Criteria for predicting the formation of single-phase high-entropy alloys. Phys Rev X 5: 1-6.

24. King DJM, Middleburgh SC, McGregor AG, Cortie MB (2016) Predicting the formation and stability of single phase high-entropy alloys. Acta Mater 104: 172-179.

25. Couzinié JP, Lilensten L, Champion Y, Dirras G, Perrière L, et al. (2015) On the room temperature deformation mechanisms of a TiZrHfNbTa refractory high-entropy alloy. Mater Sci Eng A 645: 255-263.

26. Tsai MH, Li JH, Fan AC, Tsai PH (2017) Incorrect predictions of simple solid solution high entropy alloys: cause and possible solution. Scripta Mater 127: 6-9.

27. Pickering EJ, Jones NG (2016) High-entropy alloys: a critical assessment of their founding principles and future prospects. Int Mater Rev 61: 183-202.

28. Senkov ON, Miracle DB (2001) Effect of the atomic size distribution on glass forming ability of amorphous metallic alloys. Mater Res Bull 36: 2183-2198.

29. Ji X (2015) Relative effect of electronegativity on formation of high entropy alloys. Int J Cast Metal Res 28: 229-233.

30. Guo S, Ng C, Lu J, Liu CT (2011) Effect of valence electron concentration on stability of fcc or bcc phase in high entropy alloys. J Appl Phys 109: 1-5.

Author Affiliation   *Top*

Department of Materials Science and Engineering, University of Ioannina, 45110, Ioannina, Greece